

We are IntechOpen, the world's leading publisher of Open Access books Built by scientists, for scientists

6,900

Open access books available

186,000

International authors and editors

200M

Downloads

Our authors are among the

154

Countries delivered to

TOP 1%

most cited scientists

12.2%

Contributors from top 500 universities



WEB OF SCIENCE™

Selection of our books indexed in the Book Citation Index
in Web of Science™ Core Collection (BKCI)

Interested in publishing with us?
Contact book.department@intechopen.com

Numbers displayed above are based on latest data collected.
For more information visit www.intechopen.com



Nitrogen-Containing Carbon Nanotubes - A Theoretical Approach

M. Leonor Contreras and Roberto Rozas

*University of Santiago de Chile, Usach, Faculty of Chemistry and Biology
Chile*

1. Introduction

Carbon nanotubes are important materials for a variety of scientific and technological applications due to their unique properties (Frank et al., 1998; Ganji, 2008; Hone et al., 2000; Marulanda, 2010; Yu et al., 2000). Of course, their properties depend on their structure. For instance, nanotube conductivity depends on chirality, diameter, and length (Alam & Ray, 2007; Hamada et al., 1992; Saito et al., 1992; S.H. Yang et al, 2008). The purity of the nanotubes and the presence of defects also affect their conductivity.

Chirality or helicity refers to the way the nanostructure arises by the folding of a graphene sheet. Nanotube chirality is usually characterised by two integers, n and m , known as Hamada indices, defining three classes of nanotubes. For instance, *armchair* (n,n) nanotubes exhibit metallic behaviour, *zigzag* ($n,0$) nanotubes are semiconductors, and *chiral* (n,m) nanotubes exhibit metallic behaviour if the difference ($n - m$) is a multiple of 3 and semiconductor behaviour otherwise (Charlier, 2002). For instance, a ($7,1$) *chiral* nanotube is a conductor but the *chiral* ($7,3$) nanotube is not.

Within the numerous potential applications imagined for carbon nanotubes, hydrogen storage represents the most promising application capable of making a safe, efficient and “green” contribution to fuel cells with hydrogen management in the solid state. The principal hydrogen-adsorption mechanisms associated with nanotube hydrogen uptake are the physisorption and chemisorption of hydrogen.

During physisorption, hydrogen interacts with selected sites of a carbon nanotube or substrate. The interaction energy increases as the substrate polarisability increases. Density-functional theory calculations indicate that nanotube-hydrogen interactions are weak and that hydrogen diffusion from the nanotube is facilitated by slightly increasing temperature (Mpourmpakis et al., 2006). The hydrogen-binding energies, calculated using density-functional theory are small and similar for metallic and semiconducting nanotubes, indicating that substantial adsorption is only possible at very low temperatures (Cabria et al., 2006). The same conclusion is reached by studying hydrogen adsorption in carbon-nanotube arrays through molecular dynamic simulation (Kovalev et al., 2011), in which a second adsorption layer is detected at 80 °K. This second layer of hydrogen is not detected at room temperature.

Through chemisorption, hydrogen is covalently bonded to carbon atoms in such a way that a change of sp^2 to sp^3 carbon hybridisation occurs, which is manifested in the C–C bond length values. A typical (sp^3)C–C(sp^3) bond length is 1.54 Å. The calculated C–C bond

lengths for fully hydrogenated nitrogen-containing carbon nanotubes, obtained using density-functional theory, are somewhat longer and range from 1.54 to 1.57 Å (Contreras et al., 2010) depending on the nanotube configuration.

Experimental work by Dillon et al. (Dillon et al., 1997), which reported 10 wt. % of hydrogen uptake by single-walled carbon nanotubes at room temperature, stimulated many theoretical and experimental studies of carbon nanotubes as an ideal hydrogen carrier (Bilic & Gale, 2008; Dinadayalane et al., 2007; Kaczmarek et al., 2007). The hydrogen binding energies in these cases are clearly dependent on chirality, tube diameter, hydrogen occupancy, and endohedral vs. exohedral binding.

For example, based on density-functional theory calculations of atomic hydrogen adsorption on carbon nanotubes at very low occupancies (i.e., 1 or 2 adsorbed hydrogen atoms), F.Y. Yang et al. reported that the binding energies for *zigzag* nanotubes increase as the nanotube diameter increases and are higher than the binding energies for *armchair* nanotubes (F.H. Yang et al., 2006). In contrast, calculations for *armchair* nanotubes by Dinadayalane et al. at the same level of density-functional theory showed that binding energy (or exothermicity) of hydrogen chemisorption decreases as the nanotube diameter increases (Dinadayalane et al., 2007). However, for a single hydrogen atom adsorbed on a single-walled-carbon-nanotube surface, density-functional theory calculations indicate that both the binding energy (chemisorption) and the diffusion barrier for a hydrogen atom decrease as the tube diameter increases (Ni & Zeng, 2010). In this case, the binding energy is not strongly affected by the tube chirality (Ni & Zeng, 2010).

It is clear that exohedral binding is more energetically favourable than endohedral binding because the conversion of sp^2 to sp^3 hybridisation upon hydrogen binding is easier for the carbon atoms of the exterior carbon-nanotube walls (F.H. Yang et al., 2006). It is also apparent that adsorbed hydrogen acts as an autocatalyst for further hydrogenation, as was reported by Bilic and Gale after investigating the chemisorption of molecular hydrogen on small-diameter *armchair* carbon nanotubes using density-functional theory (Bilic & Gale, 2008). Bilic and Gale found that only small-diameter nanotubes (diameters up to 10 Å) have the theoretical potential for a high hydrogen uptake by chemisorption (Bilic & Gale, 2008).

However, from a quantitative viewpoint, some of the experiments performed at room temperature resulted in very low hydrogen-storage capacities, generating debate and much controversy (Baughman et al., 2002; G. Zhang et al., 2006). Density-functional theory calculations of both the energy-barrier and the Gibbs-free-energy changes for hydrogen on a (10,0) single-walled carbon nanotube when changing from a physisorption to a chemisorption state (Han & Lee, 2004) suggest a major obstacle for the practical use of the carbon nanotube as a hydrogen storage medium.

Several research groups' results have indicated that hydrogen uptake depends on factors, such as the nanotube type and purity, the gas temperature and pressure, and the equipment used for the experimental determination, all of which affect reproducibility. A recent detailed discussion by Yao (Yao, 2010) about different experimental and theoretical studies critically analyses the influencing factors that must be considered for a better evaluation of carbon nanotubes as good candidates for hydrogen storage. Two important points mentioned are the nanotube purity after synthesis and the presence of some heteroatoms that could modify the nanotube surface electronic density.

Using a volumetric measurement setup specifically designed for carbon nanotubes, Liu et al. obtained results for different types of nanotubes, showing that the reliable hydrogen storage capacity of carbon nanotubes under a pressure of approximately 12 MPa at room

temperature is less than 1.7 wt. % (Liu et al., 2010). This value is far below the benchmark of 6.5 wt. % set by the US Department of Energy for the on-board application of hydrogen storage systems, suggesting that hydrogen uptake in pure carbon nanotubes is not a good alternative for on-board applications.

Doping is also an important factor to consider (Griadun, 2010). Semiconducting carbon nanotubes doped with 2–10% of nitrogen become metallic (Charlier, 2002; Czerw et al., 2001). Interestingly, nitrogen-doped carbon nanotubes constitute a good metal-free catalyst system for oxygen reduction reactions in alkaline media (Gong et al., 2009). In acidic media, these nitrogen-doped carbon nanotubes show a higher current density and a higher oxygen reduction reaction rate constant compared to conventional Pt-based catalysts (Xiong et al., 2010). Nitrogen-doped carbon nanotubes behave as convenient catalysts for these reactions and have excellent environmental and economical profiles because they are electrochemically more reactive and more durable than Pt-containing materials. Density-functional theory calculations at the B3LYP/6-31G* level indicate that the metal-free nitrogen-doped carbon nanotubes have promising catalytic ability for C-H methane activation (Hu et al., 2011) that is comparable to that of noble-metal catalysts and enzymes.

In addition, the nitrogen doping of carbon nanotubes has a significant effect on hydrogen storage capacity. Density-functional theory calculations for atomic hydrogen adsorption indicate that nitrogen-doping forms an electron-rich six-membered ring structure and decreases the adsorption energies in single-walled carbon nanotubes (Zhou, et al., 2006). Nevertheless, doping nanotubes with nitrogen considerably enhances the hydrogen dissociative adsorption, substantially reducing the hydrogen diffusion barrier according to density-functional theory studies on nitrogen-doped (8,0) nanotubes (Z.Y. Zhang & Cho, 2007).

Hydrogen molecules can diffuse inside nitrogen-doped *zigzag* (10,0), *chiral* (7,5) and *armchair* (6,6) nanotubes (with diameters of approximately 8 Å), as indicated by molecular dynamics simulation (Oh et al., 2008), suggesting that these nitrogen-doped nanostructures could be applied as effective media for the storage of hydrogen molecules. However there has not been any publication estimating the amount (wt. %) of hydrogen uptake achieved by these nitrogen-doped nanotubes. Importantly, most of these studies are conducted only for structures with small nitrogen content. Research on the adsorption of molecular hydrogen on the external surface of single-walled (8,0) nanotubes decorated with atomic nitrogen (approximately 14.6 wt. % of nitrogen content) using both density-functional theory and molecular dynamics found that the system can store up to 9.8 wt. % of hydrogen at 77°K (Rangel et al., 2009) and that 6.0 wt. % of hydrogen remains adsorbed at 300°K at ambient pressure with an average adsorption energy of $-80 \text{ meV}/(\text{H}_2)$. These results suggest that nanotubes with higher nitrogen content could potentially constitute a high-capacity hydrogen storage medium.

Experimental measurements on hydrogen storage associated with other nitrogen-doped carbon structures indicated that nitrogen-doped microporous carbon had both an 18% higher hydrogen-storage capacity and significantly higher heats of hydrogen adsorption than a pure carbon structure with a similar surface area (L.F. Wang & R.T. Yang, 2009). In addition, nitrogen-doped carbon xerogels enhanced hydrogen adsorption at 35°C (K.Y. Kang et al., 2009).

Because the incorporation of nitrogen atoms into carbon nanotubes affords structures with the ability to participate in hydrogen bonding, these nitrogen-doped nanostructures may have additional chemical properties, such as the immobilization of transition metals (Feng et

al., 2010), or the coupling of gold nanoparticles (Allen et al., 2008), which could be useful for potential biomedical applications.

Nitrogen-doped nanotubes are less toxic than undoped carbon nanotubes, but some concern about their safe use remains (Pastorin, 2009; Stern & McNeil, 2008). Experimental research involving the analysis of the toxicological effects on both mice and amoeba cell viability caused by nitrogen-doped or undoped carbon nanotubes indicates that nitrogen-doped carbon nanotubes are less harmful and more biocompatible than the undoped nanotubes (Terrones, 2007).

For undoped carbon nanotubes, a recent scientific study (Nayak et al., 2010) investigated a variety of parameters concerning the toxicity of either single- or multi-walled carbon nanotubes, with and without functionalisation, to assess their cytotoxic profile; this assessment was based on several critical parameters, such as tube length, concentration, dispersibility, and purity, using colorimetric assays to measure the activity of mitochondrial reductase. The results of these studies show that the purity and dispersibility of the nanotubes are the most critical parameters to guarantee their safe application in biology and medicine when used in a normal concentration range (10-150 $\mu\text{g}/\text{ml}$). This finding is an important contribution to the field, assuring the safe use of ultrapure nanotubes.

All of the aforementioned features make the study of the properties, stability and hydrogen chemisorption energies of carbon nanotubes with high nitrogen content quite interesting and necessary. As an extreme, nitrogen nanotubes or nitrogen nanoneedles formed by units of N_{2m} ($m = 2-6$) with hydrogen as the terminal atoms (with almost 100 wt. % of nitrogen) as well as nitrogen nanobundles with a carbon backbone have been studied using the density-functional theory method (J.L. Wang et al., 2006). J.L. Wang et al. reported that the mentioned nitrogen nanostructures and the nitrogen nanobundles have low stability but are proper minima with all real frequencies at the level of B3LYP/6-31G** having electronic properties that might be modulated as a function of the local charge environment.

There are only a few studies on nitrogen-containing carbon nanotubes with high nitrogen content. However, the synthesis of nitrogen-doped carbon nanotubes (Trasobares et al., 2002) can be selectively performed with either sp^2 or sp^3 nitrogen atoms (Zhong et al., 2007), and nitrogen configuration can be controlled during the fabrication of the nitrogen-doped carbon nanotubes to obtain the desired nanotube properties (S.H. Yang et al., 2008). Nitrogen-doped carbon nanotubes with different nitrogen contents synthesised by chemical vapour deposition (CVD) with pyridine as the nitrogen source and acetylene as the carbon source contain pyridinic, pyrrolic and graphitic types of C-N bonds, as revealed by X-ray photoelectron spectroscopy (XPS) (Y. Zhang et al., 2010).

Fully exohydrogenated nitrogen-containing carbon nanotubes with high nitrogen content, having sp^3 nitrogen atoms, have been reported to be stable compounds (Contreras et al., 2010) with promising expected properties that have not yet been fully studied.

Our aim in this work is to theoretically investigate the structural geometry, energetic stabilities, and electronic properties and to calculate the hydrogen-chemisorption energy for a particular family of nitrogen-containing carbon nanotubes using the density-functional theory method at the B3LYP/6-31G* level of theory. These nanotubes have very small diameters (≈ 0.3 nm) and a C_4N_2 cyclic unit with a pyrimidine-like disposition as the repetitive layer (with 36-37 wt. % nitrogen content). We also would like to clarify whether their structural and electronic properties are affected by the presence of different terminating units at the nanotube ends. The final aim of this work is the evaluation of the possibility that these nitrogen-containing carbon nanotubes behave as hydrogen-storage

materials and to determine the influence of both the nanotube configuration and length on their properties.

2. Computational methodology

In this work, chemisorption refers to exhaustive chemisorption with completely saturated products. The full exohydrogenated nanostructures were built using the HyperChem v7.0 program (Hyperchem, release 7.0), starting from layers defined as cyclic units containing four sp^3 carbon atoms and two sp^3 nitrogen atoms forming a pyrimidine-like framework (nitrogen atoms are separated by a single carbon atom, -N1-C2-N3-C4-C5-C6-, as shown in Figure 1). The previous visualisation of nitrogen doping for different nanotube configurations was performed using a specially designed *ad hoc* graphical interface (Contreras et al., 2009).

Nanostructures were built by covalently arranging one layer on top of the other in such a way that the carbon and nitrogen atoms were sp^3 -hybridised, thus forming open-ended nanotubes terminated with hydrogen atoms oriented parallel to the nanotube primary axis. Different configurations were characterised according to the rotation angle between adjacent layers, giving *S*, *O*, *M*, and *P* configurations for rotation angles θ of 0° , 60° , 120° , and 180° , respectively (*O*, *M*, and *P* were chosen based on the *ortho*, *meta*, and *para* positions of disubstituted benzene rings, with carbon atom number 2 taken as a reference, as shown in Figure 2).

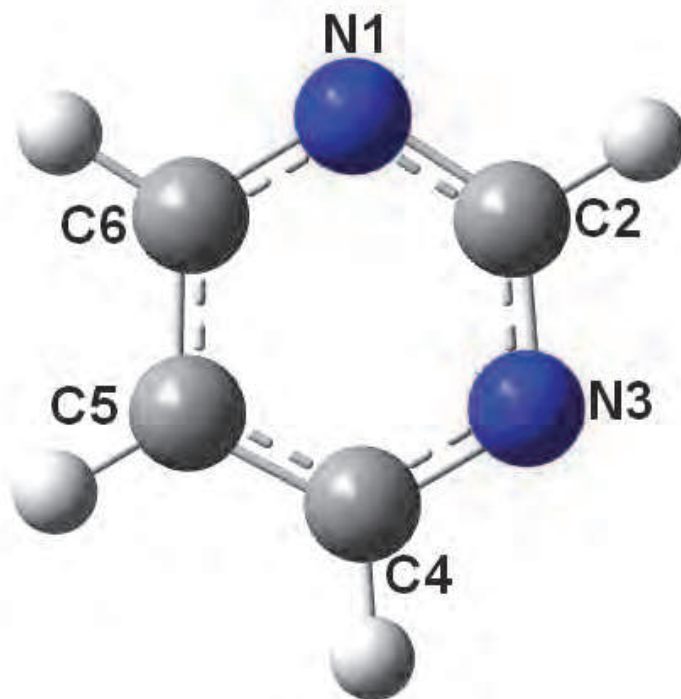


Fig. 1. Representation of the cyclic unit used as framework for building up the nitrogen-containing carbon nanotubes. Carbon atom denoted as C2 is used as reference for defining nanotube configuration.

All nanostructures were optimised by the density-functional theory (DFT) method at the B3LYP/6-31G* level of theory (Becke, 1993; Lee et al., 1988) using the Gaussian 03 suite of programs (Frisch et al., 2004). For the verification and characterisation of energy minima,

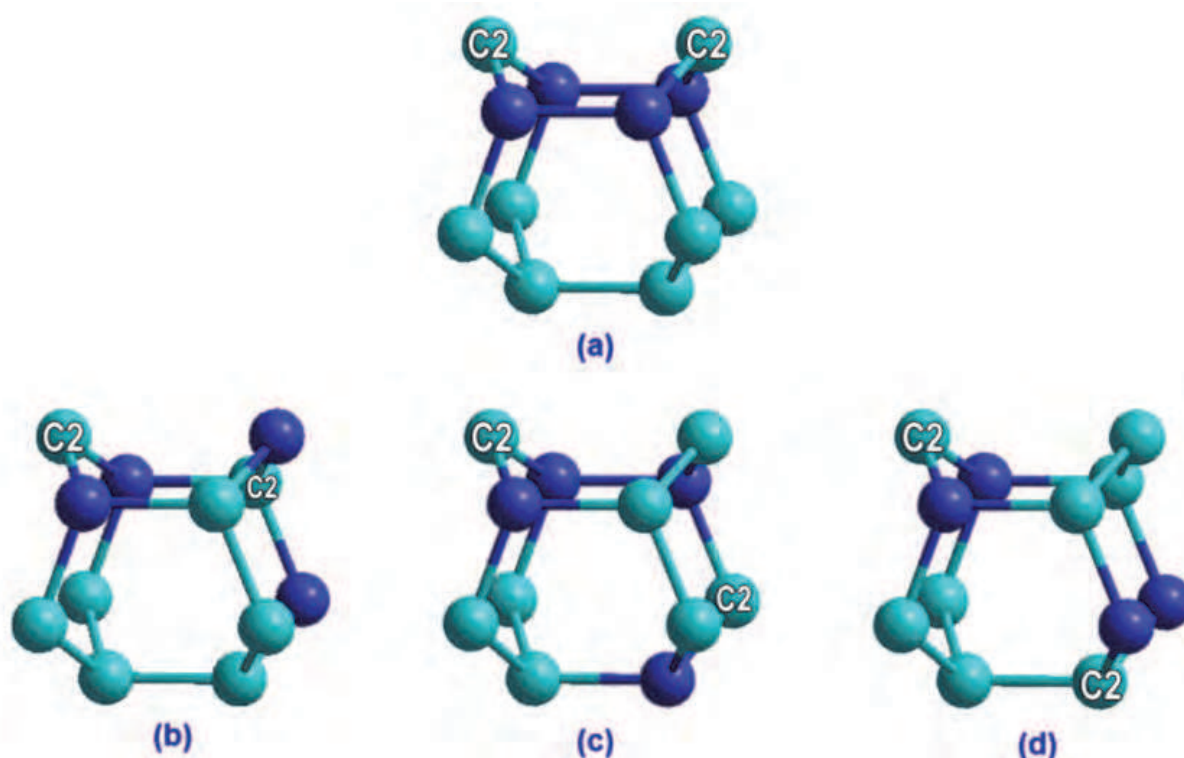


Fig. 2. Union of two consecutive layers defining the configuration of the studied nitrogen-containing carbon nanotubes. The first layer remains fixed, and the second layer is rotated. (a) eclipsed, *S*-type; (b) rotated 60° , *O*-type; (c) rotated 120° , *M*-type; (d) rotated 180° , *P*-type.

harmonic vibrational frequency calculations for optimised geometries at the same level of theory were performed, all of which yielded zero imaginary frequencies. Band gaps were calculated as the difference of $E_{LUMO} - E_{HOMO}$. No symmetry constraints were used. Charges were assigned using the Mulliken population analysis method, which partitions the total charge among the atoms in the molecule (in the present study, the sum of the Mulliken charges = 0.000 for each nanostructure).

2.1 Notation

All of the nanotubes studied in this work are nitrogen-containing carbon nanotubes with high nitrogen content, as was explained previously. Chemisorption is done to 100% hydrogen coverage.

2.1.1 Configuration

S, *O*, *M*, and *P* configurations describe the continuous rotation angle between one layer and the next, which corresponds to 0° , 60° , 120° , and 180° , respectively, as was explained above.

2.1.2 Length of the tube

This term describes the number assigned for determining how many layers or cyclic units of pyrimidinic topology are participating, which is expressed before the configuration character under consideration. For instance, 8M is assigned to a nanotube having 8 layers

with a rotation angle between contiguous layers of 120° . Different structures of 4 to 12 layers and nanotubes of up to 20 layers for some configurations have been studied.

2.1.3 Diameter

All nanostructures studied here belong to the (3,0) type with a diameter value of ≈ 0.3 nm. No variations in diameter have been considered.

2.1.4 Terminal groups

Open nanotubes ended with hydrogen atoms located coaxially to the nanotube were studied. The orientation variation of these hydrogen atoms may affect the total energy of the nanotube up to ≈ 50 kcal/mol (Contreras, et al., 2010; J.L. Wang et al., 2006). The effect of the terminal groups created by changing the three terminal hydrogen atoms by one unit of nitrogen, phosphorus, NO_3 group or a cycle of five carbon atoms (designated as 5C) at each end of the nanotube was also studied. In this way, the nanotubes remain closed at both extremes.

2.1.5 Chemisorption

A capital letter H is added to the name of the terminal group for nanotubes with adsorbed hydrogen (chemisorbed). The considered nanotubes have both extremes symmetrically bonded. In this way, a nanotube of 8 layers with an M configuration with chemisorbed hydrogen and with nitrogen as the terminal group at both extremes is designated as 8M-N-H. With no hydrogen chemisorption, the notation of 8M-N is used. If there are also no terminal groups that are different from hydrogen, the nanotube is designated simply as 8M. Therefore, in general terms, the notation is

$$(\text{number of layers}) (\text{configuration})\text{-(terminal groups)}\text{-(w/out hydrogen adsorption)} \quad (1)$$

Chemisorption, when present, is exhaustively considered with the formation of completely saturated nanostructures. Therefore, a saturated nanotube in this work is a nanotube for which hydrogen chemisorption occurred exhaustively.

2.1.6 Further calculations

Calculations for nanotubes with 20 layers (206 atoms and 1972 basis functions) were conducted using the Jaguar v7.5 (Jaguar, 2008) and the DFT method at the B3LYP/6-31G* level of theory (Becke, 1993; Lee et al., 1988); with the Gaussian 03, it was not possible to optimise these structures after several days of computation.

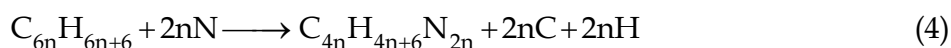
Formation energies (or substitution energies) were calculated as

$$E_{\text{Form}} = E_{\text{NCNT}} + 2nE_{\text{C}} + 2nE_{\text{H}} - E_{\text{CNT}} - 2nE_{\text{N}} \quad (2)$$

where E_{NCNT} and E_{CNT} are the total energies for saturated carbon nanotubes with the same number of layers with and without nitrogen, respectively; E_{C} , E_{H} , and E_{N} are the total energies of an isolated carbon atom, hydrogen atom, and nitrogen atom, respectively; and n is the total number of layers in the nanotube. E_{C} was calculated as

$$E_{\text{C}} = (E_{\text{CNT}} - (6n + 6)E_{\text{H}}) / 6n \quad (3)$$

and E_H and E_N were derived from one half of the calculated total energy for a hydrogen molecule and a nitrogen molecule, respectively, at the same level of theory. For a better understanding, the process considered for a 6-layer nitrogen-containing carbon nanotube can be written as



Reaction energies for hydrogen chemisorption (E_r) on the external surface of nitrogen-containing carbon nanotubes were calculated using the formula below.

$$E_r = E_{(H \text{ chemisorbed})} - E_{(\text{without chemisorption})} - hE_H \quad (5)$$

where $E_{(H \text{ chemisorbed})}$ denotes the total energy of the hydrogen-chemisorbed nanotube; h represents the number of chemisorbed hydrogen atoms; $E_{(\text{without chemisorption})}$ and E_H correspond to the energy of sp^2 -hybridised nitrogen-containing nanotubes (ended by hydrogen atoms) and of the hydrogen atom, respectively. Expression (5) can also be written as

$$E_r = E_{C_{4n}H_{4n+6}N_{2n}} - E_{C_{4n}H_6N_{2n}} - 4nE_H \quad (6)$$

with n representing the number of layers or the length of the nanotube. E_r/H , the reaction energy per hydrogen atom, is calculated as

$$E_r / H = E_r / 4n \quad (7)$$

Some of the $C_{4n}H_6N_{2n}$ nanostructures (after being optimised to proper minima -with entirely real vibrational frequencies), formed small cycles at both ends of the tube in GaussView (graphical interface of Gaussian 03). To calculate E_r/H using more stable structures, nanotubes with the first and the last layers completely saturated were considered for chemisorption. Expressions (6) and (7) remain, respectively, as the following (8) and (9) expressions:

$$E_r = E_{C_{4n}H_{4n+6}N_{2n}} - E_{C_{4n}H_{14}N_{2n}} - (4n - 8) E_H \quad (8)$$

$$E_r / H = E_r / 4n - 8 \quad (9)$$

3. Results and discussion

Results will be presented in sections following the indicated order. First, the results obtained for completely hydrogenated open nitrogen-containing nanotubes and ended by hydrogen atoms will be shown, which represent 100% chemisorption. Next, the effect of closing the open nanotubes with different terminal groups will be shown. The results for the nanotubes without chemisorption will follow. Finally, the calculated energies of chemisorption will be presented.

3.1 Geometrical structures

The considered fully hydrogenated nitrogen-containing carbon nanotubes formed by $C_4N_2H_4$ units and ended by hydrogen atoms are ≈ 0.28 nm in diameter and 0.66–3.96 nm in

length. The interlayer bond lengths calculated by density-functional theory for N–N, N–C, and C–C bonds are 1.52 Å, 1.48–1.50 Å, and 1.55–1.56 Å, respectively. A typical (sp³)C–C(sp³) bond length is 1.54 Å. The C–N bond length for amines is 1.479 Å. The N–N bond length in nitrogen nanotubes calculated at the density-functional theory level range from 1.42 to 1.52 Å (J.L. Wang et al., 2006).

To analyse the bond lengths and bond angles inside each nanotube layer, all nanotube geometries were optimised at the same level of theory, including pyrimidine and its saturated isomer as a reference. Based on the comparison of the bond angles and bond lengths of pyrimidine and its saturated isomer, the saturated structure has smaller bond angles and higher bond lengths than pyrimidine, as was expected for these structures (see Figure 3).

To analyse the same parameters for nanotubes, an 8M (8 layers, with M configuration) nanotube was selected at random and only layer 2 and layer 4 were considered for the analysis of both the nanotube without hydrogen adsorption (8M-H) and the totally saturated (8M-H-H) nanotube (see Figure 4).

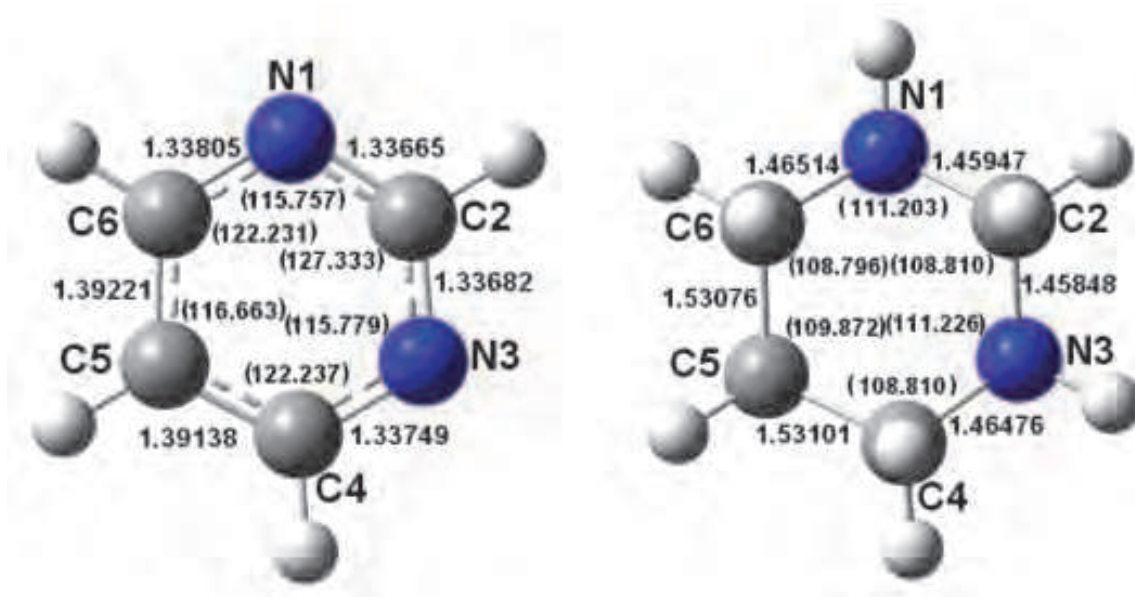


Fig. 3. Optimised geometry data for the structures of pyrimidine (left) and its saturated isomer (right). Bond lengths (in Å) are written outside of the cycle, while bond angles are written in brackets inside the cycle.

For the saturated 8M-H-H nanotube, a good correlation is observed among layers 2 and 4 when the C–C and C–N bond lengths and bond angles are compared. However, for the 8M-H nanotube, there is no a good correlation for these values. These results may be explained by the fact that saturated structure environments around layers 2 and 4 are more similar, and thus the characteristics of the layers along the tube are likely to be maintained. However, for the unsaturated structure, layer 2 is nearest to layer 1, which has three covalent bonds to hydrogen atoms, compared to layer 4, which has no neighbours bonded to hydrogen. Based on the analysis of the intralayer parameters, there is only one pair of C–C bonds in layer 2 that are longer for the saturated structure than those for the unsaturated one. Instead, in layer 4, there are several bonds in the saturated structure that are longer than those in the unsaturated one (except for the N1–C2 and N3–C4 bonds).

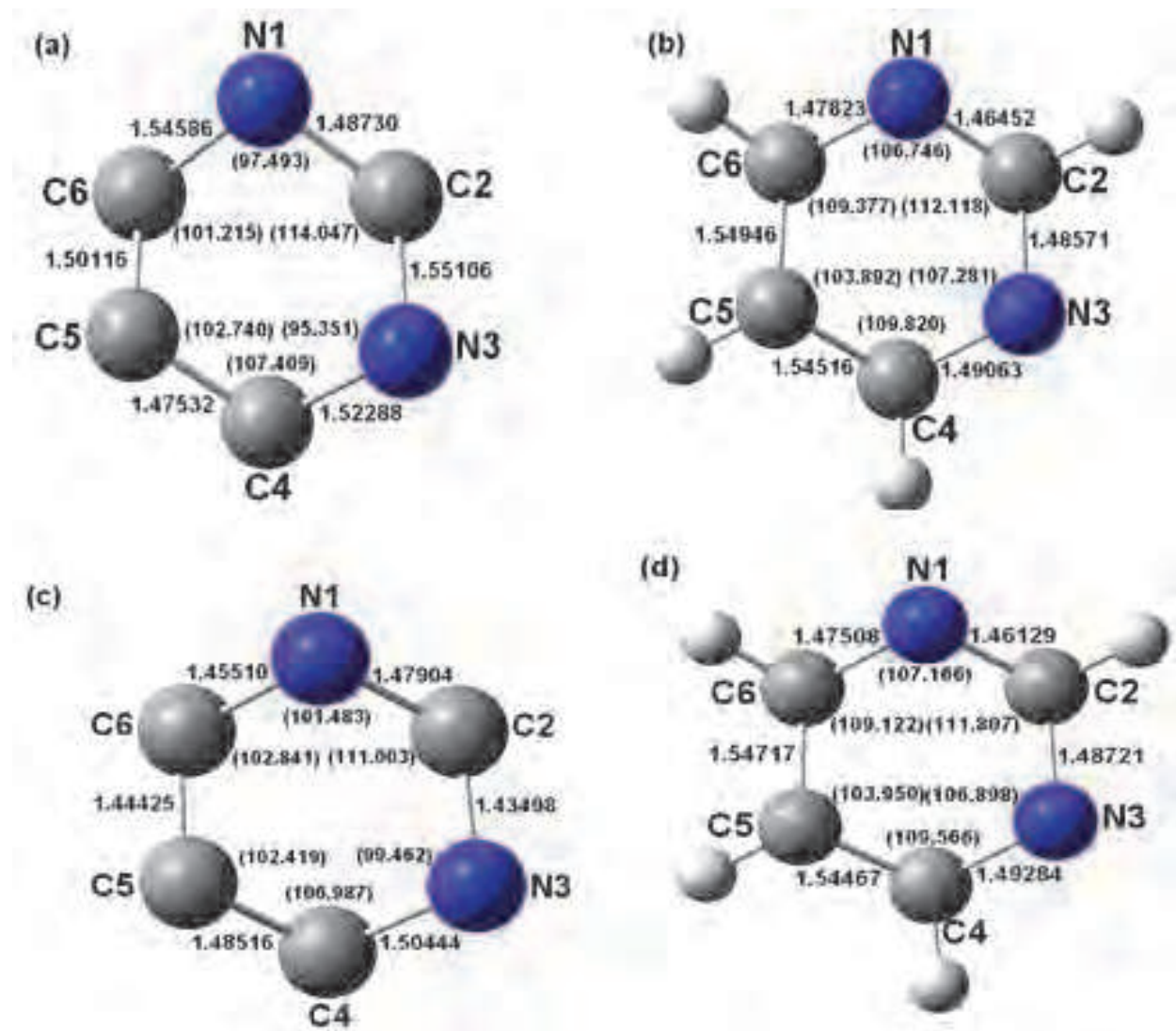


Fig. 4. Structural characteristics for the second (a, b) and fourth (c, d) 8M-nanotube layers: (a and c) without hydrogen chemisorption and (b and d) with hydrogen chemisorption. Bond lengths (in Å) are written outside of the cycle, while bond angles are written in brackets inside the cycle.

3.2 Formation energies

The formation energies of the nitrogen-containing carbon nanotubes were calculated using the density-functional theory method at the B3LYP/6-31-G* level and equation (2). Figure 5 shows the values obtained for nitrogen-containing carbon nanotubes that were totally hydrogenated with different configurations as a function of nanotube length.

A clear difference in stability for different configurations can easily be seen, with an expected regular trend of increasing formation energy as the nanotube length increases. The *O*-configuration is the most stable (with formation energies between 1.95 and 13 eV for nanotubes having between 2 and 10 layers and a formation energy of 30.45 eV for a nanotube of 20 layers -not seen), followed closely by the *P*-configuration. The *S*-configuration is the most unstable (with formation energies between 4 and 24 eV for nanotubes of 2-10 layers long and 53.16 eV for a 20-layer nanotube -not seen), and the *M*-

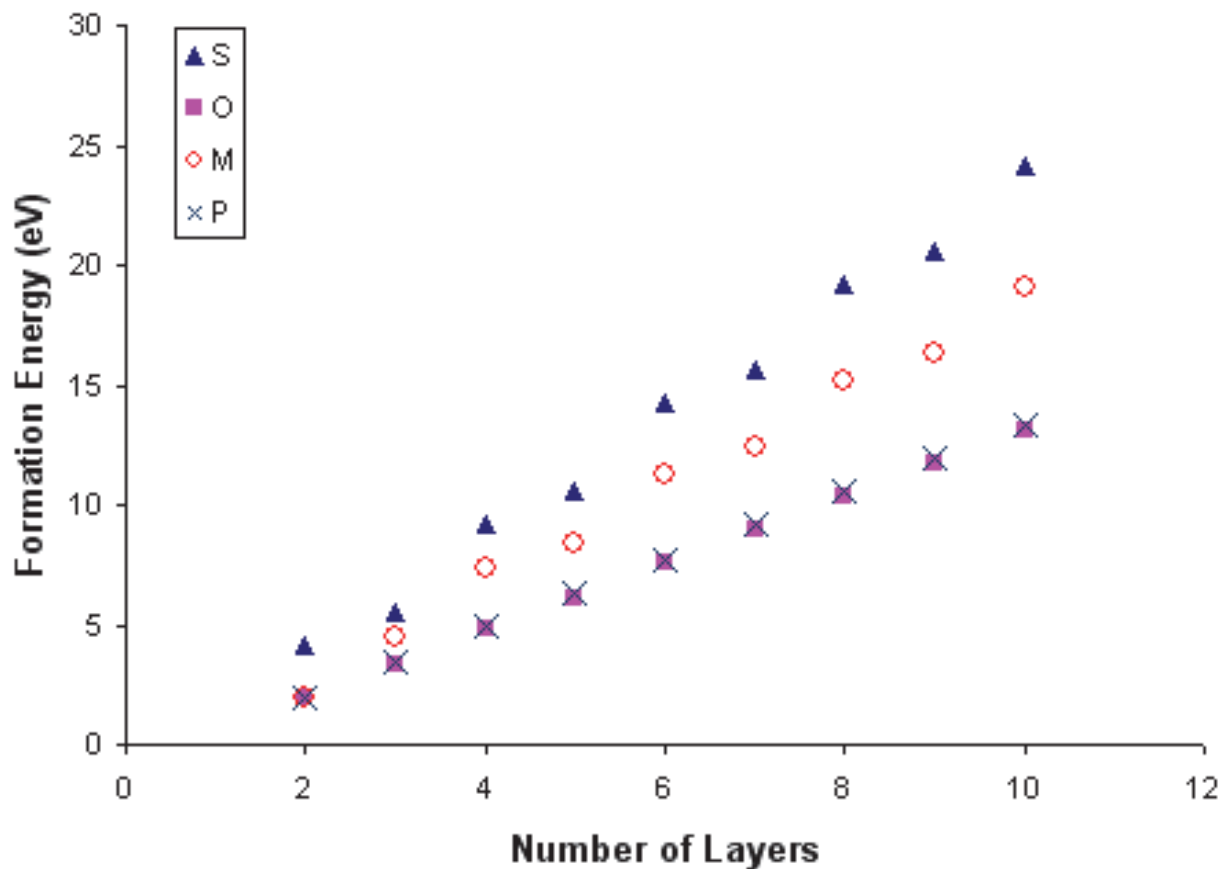


Fig. 5. Formation-energy values for saturated nanotubes of different configurations as a function of length.

configuration was of intermediate stability. For undoped carbon nanostructures of the type $H_3(C_6)_mH_3$ with $m=3-6$, values equivalent to 8–43 eV have been reported (J.L. Wang, et al., 2006), as calculated using density-functional theory methods. For a nitrogen-doped (5,5) nanotube ($C_{74}N_6$) with a diameter of approximately twice the size of those used in this work, a formation energy of 10.86 eV has been reported (H.S. Kang & Jeong, 2004). A 6O-H-H nanotube in this work, has the formula $H_3(C_4H_4N_2)_6H_3$ or $C_{24}H_{30}N_{12}$. Therefore, these systems are not directly comparable.

The formation-energy values have a close relationship to the nanotube structures in this study (see Figure 6). It is clearly observed that the S-configuration is the only configuration that has two out of the three interlayer bonds with N–N linkages. Repulsion between lone-pair-lone-pair electron clouds on the nitrogen atoms contributes to the explanation of the larger formation energies for S- and M-configurations. For M-configurations, only one of three interlayer bonds belongs to a N–N bond, which is why M-nanotubes have lower formation energies than S-nanotubes. For the O- and P-configurations, the nitrogen atoms are not bonded to each other, and the spatial disposition can be more favourable to the O-configuration to better avoid the aforementioned repulsion. Lone-pair-lone-pair repulsive interactions could also explain the observed curvature for the S-configuration of the 20-layer totally hydrogenated nanotubes, unlike those in the O-configuration (see Figure 7).

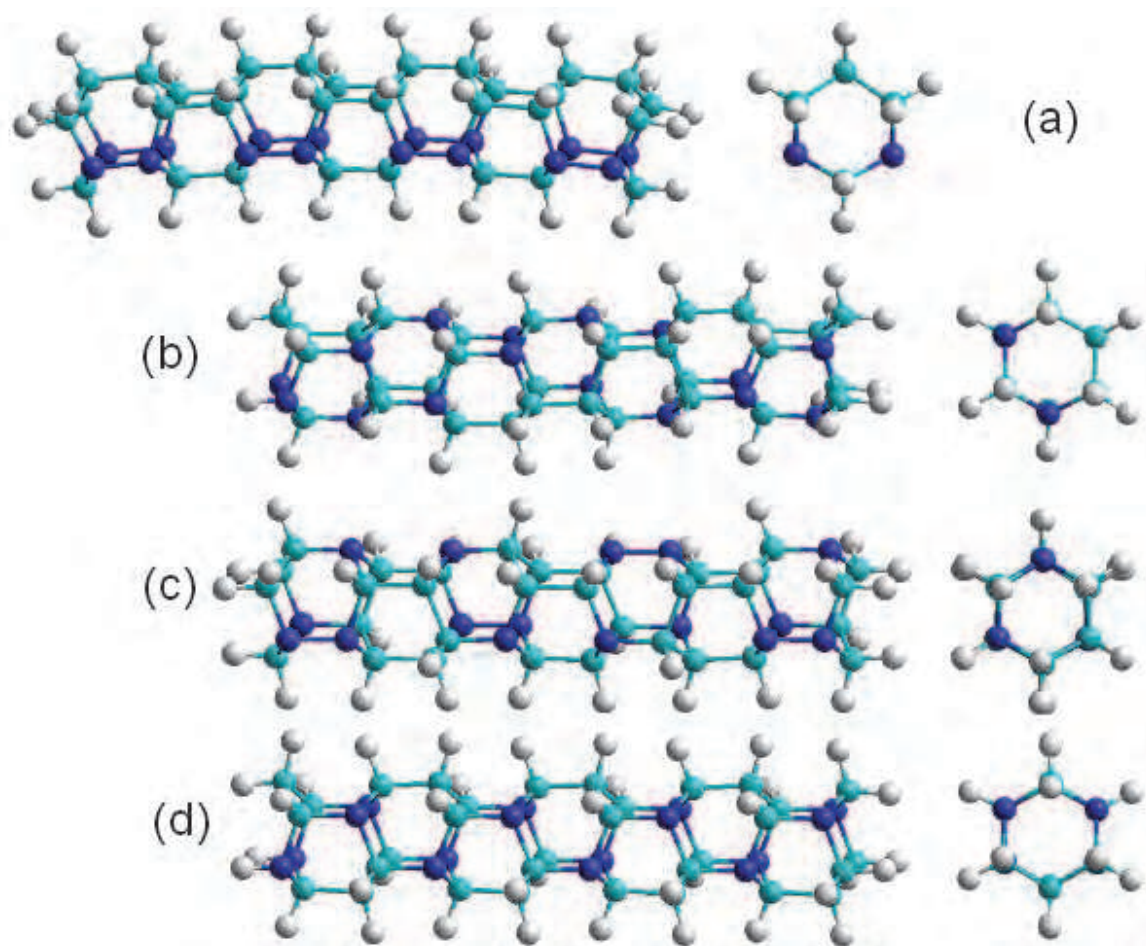


Fig. 6. Fully hydrogenated 8-layered nitrogen-containing carbon nanotubes with different configurations. (a) *S*-type, eclipsed; (b) *O*-type, rotated 60°; (c) *M*-type, rotated 120°; (d) *P*-type, rotated 180°. Top and side views of the optimised structures are shown.

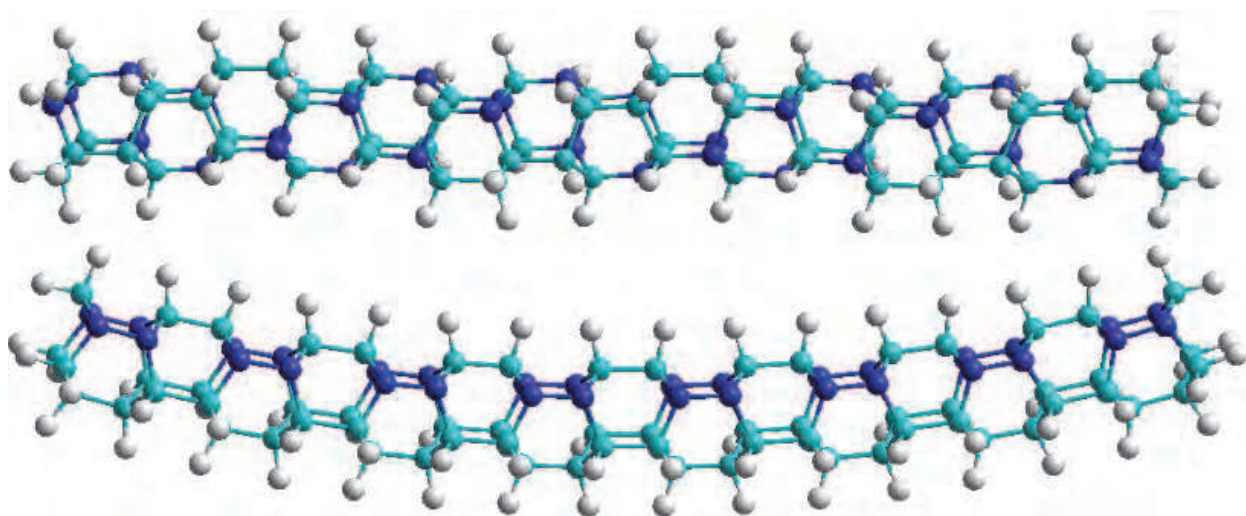


Fig. 7. Optimised geometries for the 20-layer saturated nitrogen-containing carbon nanotubes: (top) the *O*-configuration (the more stable) and (bottom) the *S*-configuration (the more unstable).

3.3 Charge analysis

Charge analysis was conducted for carbon 2 (contiguous to the two nitrogen atoms on each layer) of the most stable configuration of the hydrogen-chemisorbed nanotubes with between 1 and 10 layers. It was found that the charge value on this atom increases from the layer at the extremes of the tube up to the central layers, increasing from -0.031 for layer 1 to 0.297–0.303 for internal layers and then decreasing to 0.259–0.261 for the final layer, while charges for the nitrogen atoms remain constant at -0.481 and -0.486 for N1 and N3, respectively (Contreras et al, 2010).

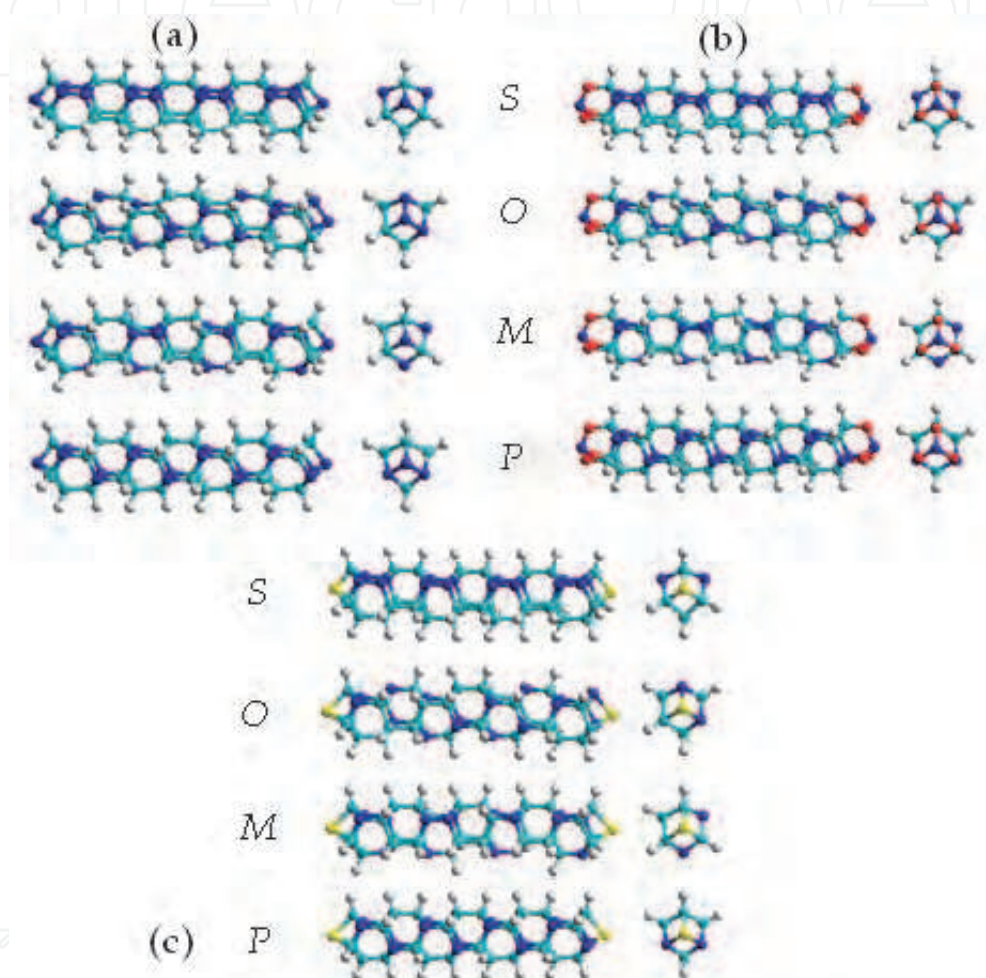


Fig. 8. Eight-layered fully hydrogenated nitrogen-containing carbon nanotubes having different configurations (*S*, *O*, *M*, and *P*) and different terminal groups. (a), (b), and (c) have the terminal groups N, NO₃, and P, respectively. Top and side views of the optimised structures are also shown.

Charge analysis clearly shows that, in the four configurations studied, the charge on C2 has a maximum value at the centre of the nanotube and that the greatest charge difference between the extremes and between one extreme and the maximum value corresponds to the *O*-configuration. Calculations indicate that structures with an *O*-configuration generate the greatest positive charge on C2, possibly because this configuration has a large number of C2 atoms linked to three nitrogen atoms, which does not occur in the other configurations. This fact could be a useful guide for oxygen reduction catalytic properties (Gong et al., 2009).

3.4 Terminal group effect

Figure 8 shows the optimised structures with all real vibrational frequencies obtained for the nanotubes containing terminal groups that close the nanotubes at both extremes as observed from the top and side views for each one.

Figure 9 shows the effect of terminal groups on the band gaps. Here, the band-gap values for nitrogen-containing carbon nanotubes are presented. Those nanotubes with chemisorbed hydrogen correspond to the group of curves above 4 eV, and the group below 4 eV is the corresponding nitrogen-containing carbon nanotubes without chemisorbed hydrogen. The nanotubes of this last group, designed by a single character H, only have hydrogen atoms in the first and in the last layers, with three hydrogen atoms on both end sides, and the nanotube is open.

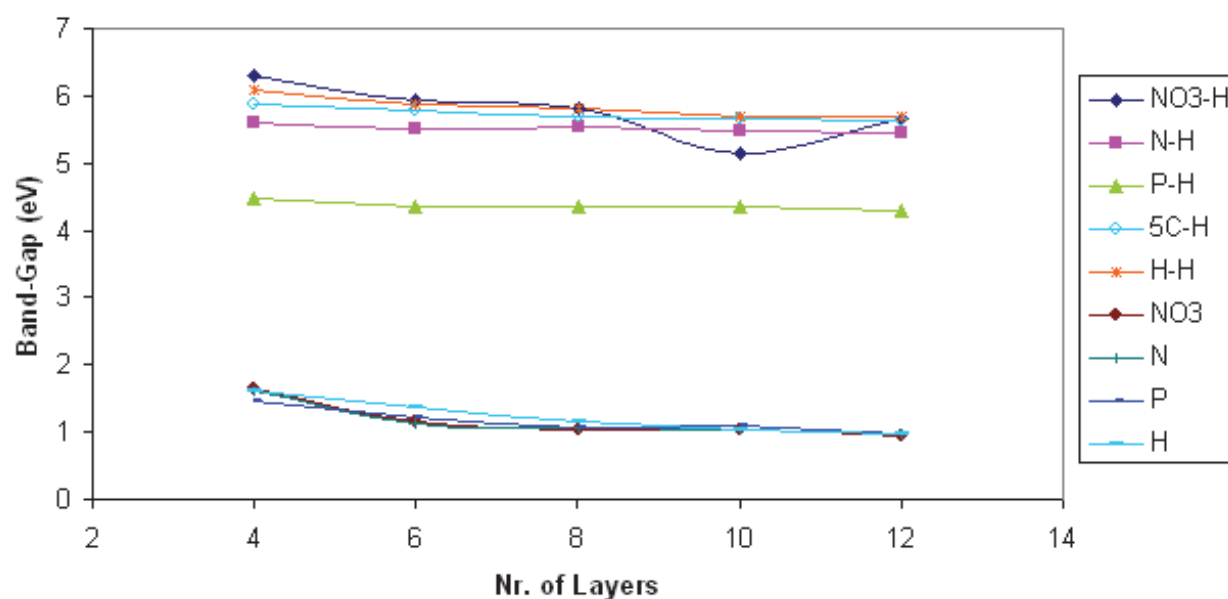


Fig. 9. Band gaps for the *M*-configuration of nitrogen-containing carbon nanotubes having different terminal groups with and without hydrogen chemisorption as a function of length. Greater values (designated by NO₃-H, N-H, P-H, 5C-H; H-H) refer to nanotubes with hydrogen adsorption. Lower values (designated as NO₃, N, P, H) do not have hydrogen chemisorbed. 5C refers to the C5-capped nanotube.

It can clearly be observed from Figure 9 that band-gap values increase for hydrogen-adsorbed nitrogen-containing carbon nanotubes having the *M*-configuration when compared with the band-gap values of the unsaturated nitrogen-containing carbon nanotubes of the same configuration. Band gaps for this last group of nanotubes with no hydrogen adsorbed are insensitive both to the terminal group and to the tube length, especially at and above 8 layers. A different situation is observed for hydrogen-adsorbed nanotubes where the band-gap values decrease by 0.4 eV and 1.6 eV, respectively, for nitrogen and phosphorus terminal groups when compared to an open nanotube with no terminal group. In general, the band gap for this group of nanotubes does not depend on the length, except for the 10-layered nanotube with a NO₃ terminal group, which has a band gap value of ≈ 0.5 eV below the value expected from the general trend.

Thus, when the unsaturated nanotube is closed by terminal groups, its semiconducting property is not strongly affected. However, results suggest that, due to hydrogen

chemisorption, the conducting property of nitrogen-containing carbon nanotubes is lost; nanotubes ending with phosphorus atoms are the least affected. This pattern was presented for the *M*-configuration but is also observed for the other studied configurations.

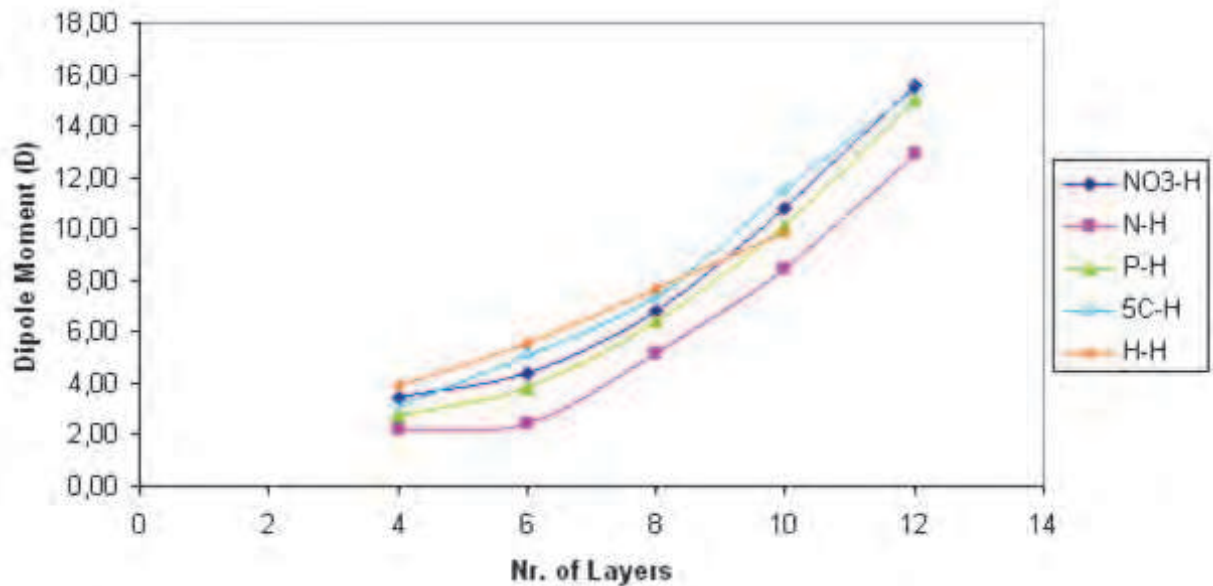


Fig. 10. Dipole moment for the *O*-configuration of hydrogen-chemisorbed nitrogen-containing carbon nanotubes with different end-groups vs. tube length.

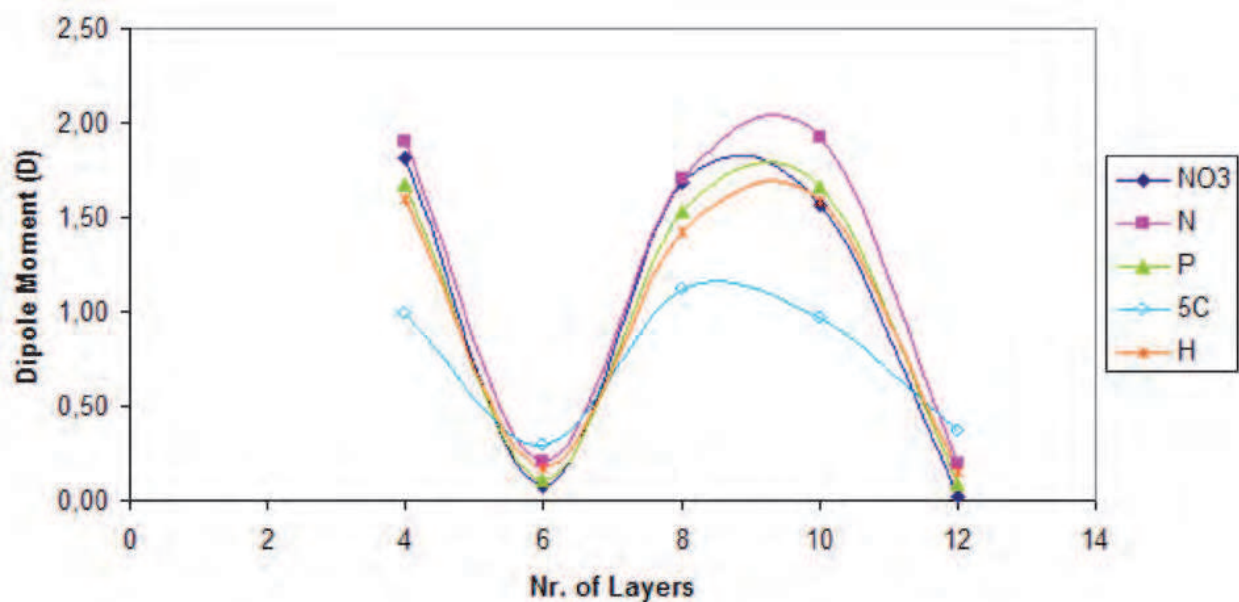


Fig. 11. Dipole moment for the *M*-configuration of unsaturated nitrogen-containing carbon nanotubes with different end-groups vs. tube length.

The terminal group effect on the dipole moment is shown for saturated nitrogen-containing carbon nanotubes with *O*-configuration at different tube lengths in Figure 10 and for unsaturated *M*-nanotubes in Figure 11. The calculated values indicate that the dipole moment clearly depends more on the tube length than on the type of terminal group, with a variation for the saturated nanotubes of within 2–3 D for the different end-groups at the

lengths considered. The respective variation for unsaturated nanotubes is less than 1 D. The dipole moment for the saturated nitrogen-containing carbon nanotubes increases with the number of layers. This trend is also true for saturated nanotubes terminated by hydrogen atoms of different configurations (Contreras et al., 2010).

Regarding the amount of hydrogen uptake by chemisorption, each terminal group replaces three hydrogen atoms at each terminus of the nanotube, and hydrogen is adsorbed at a rate of 4 atoms per layer. In this condition, nanotubes with end-groups will have a lower hydrogen uptake capacity than nanotubes without terminal groups, with values of 4.8, 4.4, and 3.7 wt. % hydrogen uptake for nanotubes ending in N, P, and NO_3 , respectively, in comparison with a 7.2 wt. % hydrogen uptake capacity for a nanotube without end-groups, with all the values being for a 4-layer nitrogen-containing carbon nanotube. Therefore, the influence of the end groups is best considered as an anchorage centre for other groups, likely being useful for further functionalisation of the nanotube with specific applications (de Jonge et al., 2005) and also facilitating physisorption because interaction with hydrogen is favoured by the donor hydrogen bond capacity of N, P, and NO_3 groups and by the increase of nanotubes polarisability in the presence of these groups. A single nitrogen atom can bind up to 6 H_2 molecules (Rangel et al., 2009).

3.5 Configuration effect

Previous analyses indicate that configuration strongly affects nanotube stability, with the *O*-configuration, in which each nitrogen atom is linked to three carbon atoms without any N–N bonds, being the most stable. It can also be observed from density-functional theory calculations that, for *S*, *M*, and *P*-configurations in general, the dipole moment increases with the nanotube length, except for the *M*-configuration, in which the dipole moment stays below 2 D independent of nanotube length and the presence of terminal groups in the structure.

The effect of nanotube configuration on the band gap for 8-layered nitrogen-containing carbon nanotubes with different terminal groups coming from hydrogen chemisorption is shown in Figure 12. The same behaviour is observed for nanotubes with and without terminal groups: the band gap depends very little on the configuration, except for *S*-configuration, the more unstable one, where band gap is somewhat lower than for the other configurations.

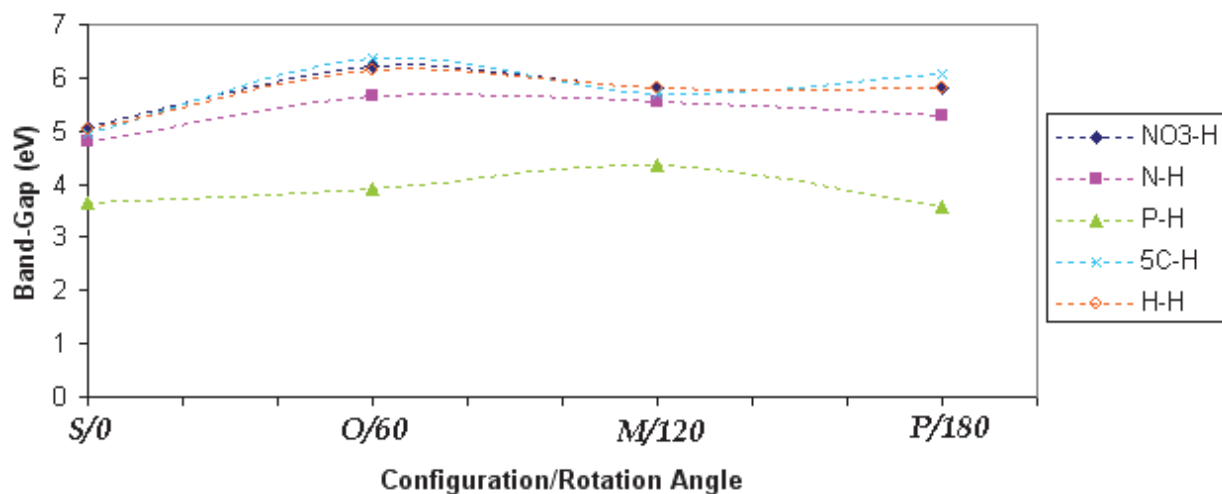


Fig. 12. Band-gap values for hydrogen-chemisorbed 8-layer nitrogen-containing carbon nanotubes with different terminal groups as a function of nanotube configuration.

The dipole moments of 8-layered nitrogen-containing carbon nanotubes for different configuration and terminal groups arising from hydrogen chemisorption are presented in Figure 13.

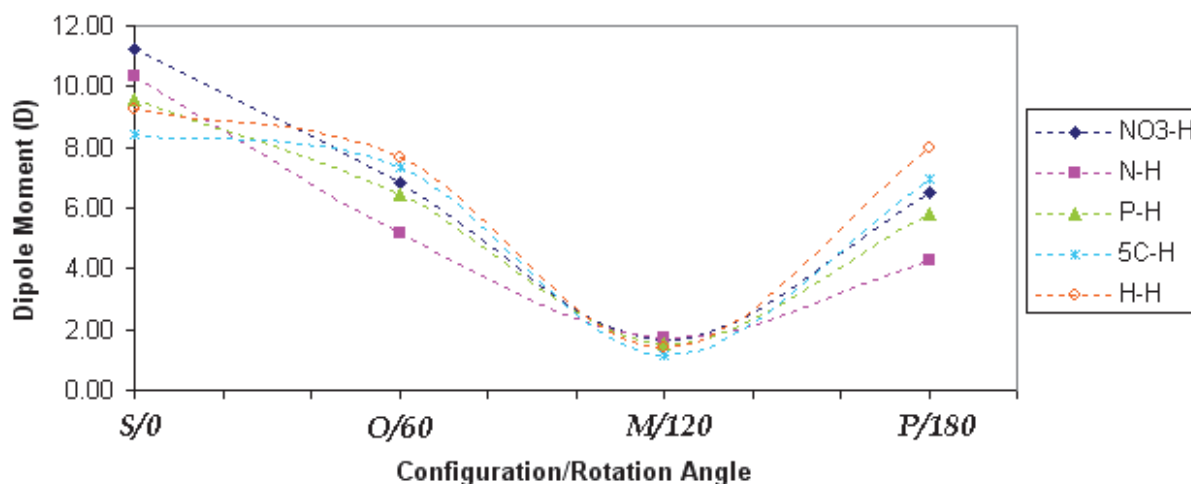


Fig. 13. Dipole moment for hydrogen-chemisorbed 8-layer nitrogen-containing carbon nanotubes with different terminal groups as a function of configuration.

Calculations using density-functional theory methods afford values indicating a configuration effect on the dipole moment for the studied nanotubes, indicating a structural relationship. For *O*- and *P*-configurations, which lack a N–N bond in their structure, the dipole moments have similar values with small differences according to the type of terminal group, decreasing from nanotubes having no terminal group in the order $H > 5C > NO_3 > P > N$. For the *S*-configurations, where two of the three interlayer bonds are N–N bonds, higher dipole moments are observed for all cases with or without terminal groups. For the case of *M*-configurations, with an interlayer rotational angle of 120° , the dipole moment does not significantly change regardless of the existence or type of functional group, being below a value of 2 D.

3.6 Hydrogen chemisorption energies

Values of hydrogen chemisorption energies for 100% saturation, calculated according to equations (6) and (7) above, for nitrogen-containing carbon nanotubes of different configurations and for carbon nanotubes of different lengths, with no terminal group, are shown in Table 1.

The energies were calculated considering the optimised geometries of the exhaustively chemisorbed nitrogen-containing nanostructures, meaning complete saturation ($C_{4n}H_{4n+6}N_{2n}$). Regular tubular structures with all real vibrational frequencies for all studied nanotube configurations and lengths were obtained. However, the optimised structures of unsaturated molecules ($C_{4n}H_6N_{2n}$), over which hydrogen adsorption takes place, showed three-membered cycles at both extremes of the nanotube with a C–C bond length of 1.51–1.53 Å and C–N bond lengths of 1.45–1.46 Å and 1.47–1.48 Å (Figure 14). These structures were optimised at the same level of theory as the previous structures, up to proper minima characterised by positive vibrational frequencies.

The values shown in Table 1 indicate that the configuration has a distinctive effect, especially on the 4-layered nanotubes. For nanotubes longer than 8 layers, there is no

significant variation of the hydrogen chemisorption energies per hydrogen atom, with configuration or length.

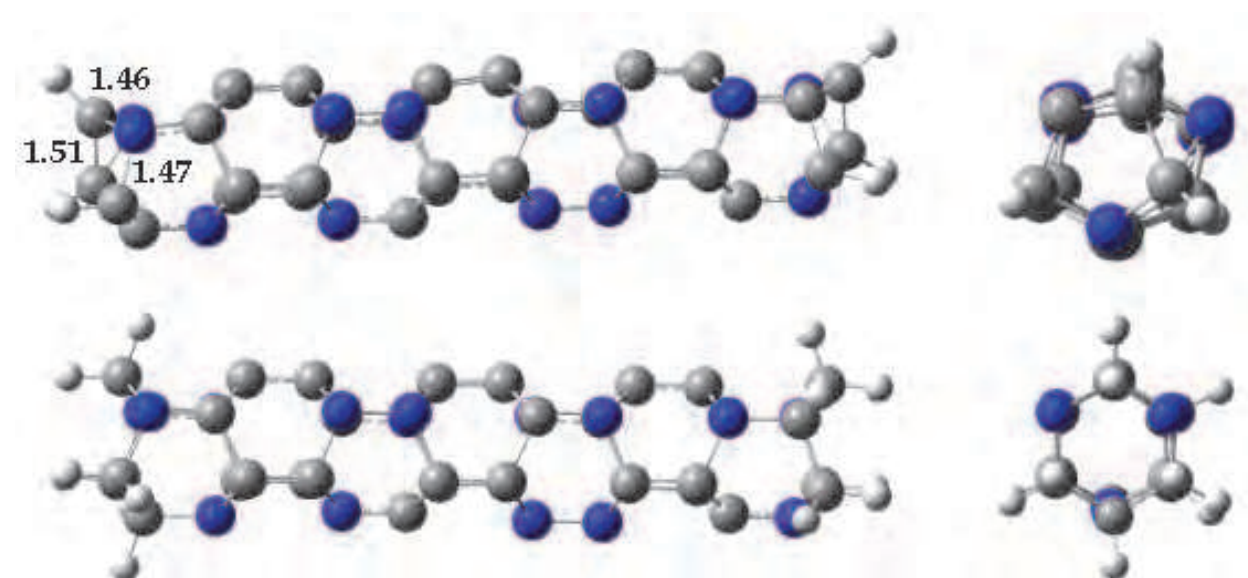


Fig. 14. Optimised structures for a 8M-nitrogen-containing carbon nanotube with no terminal group. $C_{32}H_6N_{16}$ (top) and $C_{32}H_{14}N_{16}$ (bottom). Front and side views.

configuration	Nr. of layers (n)	$E_{C_{4n}H_{4n-6}N_{2n}}$ (hartrees)	$EC_{4n}H_6N_{2n}$ (hartrees)	E_r (hartrees)	E_r/H (hartrees)	E_r/H (kcal/mol)
S	4	-1060.67372179	-1050.525874	-0.74398379	-0.046498987	-29.2
S	6	-1589.19755145	-1573.933203	-1.15855245	-0.048273019	-30.3
S	8	-2117.72125246	-2097.291591	-1.62193362	-0.050685426	-31.8
O	4	-1060.83574369	-1050.533544	-0.89833569	-0.056145981	-35.2
O	6	-1589.44157351	-1574.098557	-1.23722051	-0.051550855	-32.3
O	8	-2118.04670023	-2097.482879	-1.75609323	-0.054877913	-34.4
M	4	-1060.74319832	-1050.450297	-0.88903732	-0.055564832	-34.9
M	6	-1589.30657159	-1574.048135	-1.15264059	-0.048026691	-30.1
M	8	-2117.87029700	-2097.356125	-1.70644400	-0.053326375	-33.5
M	10	-2646.43344985	-2620.807194	-2.11659585	-0.052914896	-33.2
M	12	-3174.92435700	-3144.258419	-2.45434600	-0.051132208	-32.1
P	4	-1060.83275220	-1050.556415	-0.87247320	-0.054529575	-34.2
P	6	-1589.43566275	-1574.113497	-1.21636975	-0.050682073	-31.8
P	10	-2646.64170736	-2621.000194	-2.13185336	-0.053296334	-33.4

Table 1. Chemisorption energy values for different nitrogen-containing carbon nanotubes, with no terminal group.

Values of the hydrogen chemisorption energy for nitrogen-containing carbon nanotube structures with totally saturated first and the last layers and having the general formula $C_{4n}H_{14}N_{2n}$ are given in Table 2. In this case, the optimised regular geometries were obtained without small cycles in their structures (Figure 14).

The E_r/H values for partially saturated $C_{4n}H_{14}N_{2n}$ nanotubes are less exothermic than those obtained from less stable geometries, which was expected because less energy per hydrogen atom is to be eliminated by the exhaustive hydrogen adsorption to more thermodynamically stable molecules.

configuration	Nr. of layers (n)	E_C _{4n} H _{4n} +6N _{2n} (hartrees)	E_C _{4n} H ₁₄ N _{2n} (hartrees)	Er (hartrees)	Er/H (hartrees)	Er/H (kcal/mol)
S	4	-1060.67372179	-1055.5268440	-0.44494579	-0.02780911	-17.5
S	6	-1589.19755145	-1578.9368800	-0.85680745	-0.03570031	-22.4
S	8	-2117.72125246	-2102.3690610	-1.24639546	-0.03894986	-24.4
S	10	-2646.24491823	-2625.7817510	-1.65543923	-0.04138598	-26.0
O	4	-1060.83574369	-1055.6944090	-0.43940269	-0.02746267	-17.2
O	6	-1589.44157351	-1578.9663560	-1.07135351	-0.04463973	-28.0
O	10	-2646.65363361	-2626.2815826	-1.56432303	-0.03910808	-24.5
O	12	-3175.19965990	-3149.6779433	-2.01205660	-0.04191785	-26.3
M	4	-1060.74319832	-1055.6600322	-0.38123412	-0.02382713	-15.0
M	6	-1589.30657159	-1579.1350557	-0.76765189	-0.03198550	-20.1
M	8	-2117.87029700	-2102.6004170	-1.16408400	-0.03637762	-22.8
M	10	-2646.43344985	-2626.0716442	-1.55407765	-0.03885194	-24.4
P	4	-1060.83275220	-1055.7081300	-0.42269020	-0.02641814	-16.6
P	6	-1589.43566275	-1579.2049760	-0.82682275	-0.03445095	-21.6
P	8	-2118.03866452	-2102.7269624	-1.20590612	-0.03768457	-23.6

Table 2. Chemisorption energy values for partially saturated C_{4n}H₁₄N_{2n} nanotubes (nitrogen-containing carbon nanotubes having both the first and the last layer saturated).

The data in Table 2 indicate that, as the nanotube length increases, the hydrogen chemisorption energy increases, favouring chemisorption. The obtained values are comparable with the atomic adsorption energy of hydrogen for nitrogen-doped (8,0) carbon nanotubes with a value of -28.4 kcal/mol (Zhou et al., 2006). A strong effect of the nanotube configuration on the energy values is not observed.

Values of Er/H for hydrogen adsorption over the M-configuration of nitrogen-containing carbon nanotubes having N, P, and NO₃ terminal groups at both nanotube extremes are given in Figure 15. Calculations done by density-functional theory at the B3LYP/6-31G* level show no significant variation with the type of terminal group or nanotube length. Theoretically, only 4 hydrogen atoms per layer can be adsorbed by chemisorption.

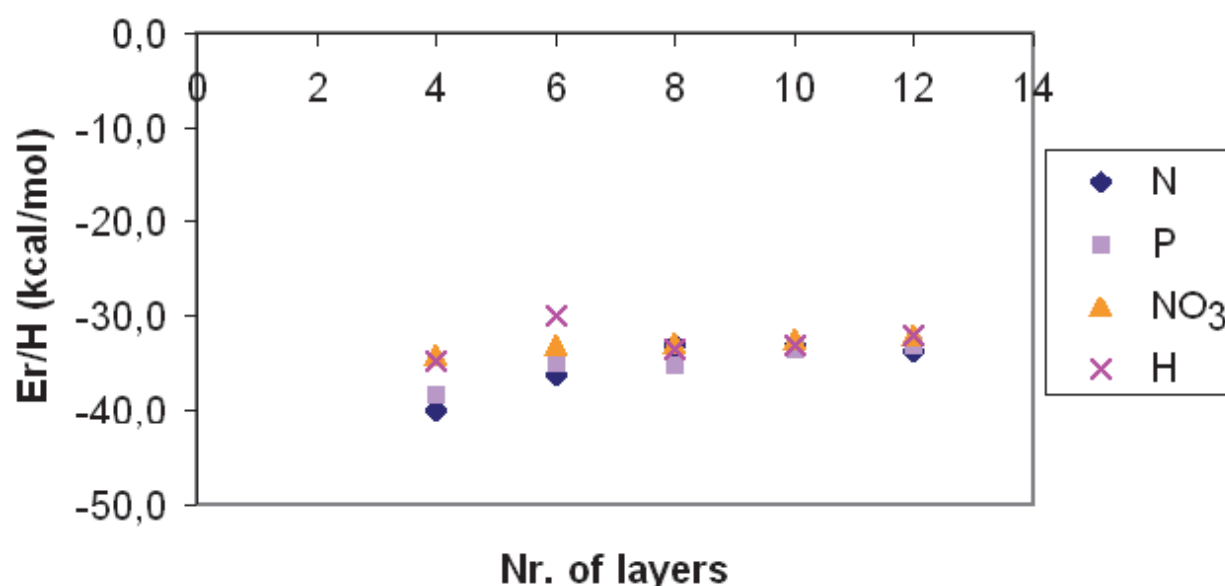


Fig. 15. Er/H values for hydrogen adsorption over nitrogen-containing carbon nanotubes of M-configuration with different end-groups vs. length.

The chemisorption process is somewhat more exothermic in the presence of terminal groups than for open nanotubes without terminal groups. The calculated molecular hydrogen absorption energy for a single-walled (8,0) carbon nanotube decorated with atomic nitrogen is also exothermic, with a value of $-80 \text{ meV}/(\text{H}_2)$, equivalent to $-1.84 \text{ kcal/mol}/(\text{H}_2)$ (Rangel et al., 2009), as determined by density-functional theory and molecular dynamics. We have not found both experimental neither theoretical studies for a more direct comparison with our results.

4. Conclusions

The structural and energy aspects of hydrogen atom chemisorption on small-diameter nitrogen-containing carbon nanotubes having high nitrogen content have been investigated. The adsorption of hydrogen was examined at full coverage. Stable nanotube structures were fully optimised to proper minima before and after hydrogen chemisorption using density-functional theory methods at the level of B3LYP/6-31G* with all real vibrational frequencies.

The stability was strongly dependant on the configuration of the saturated nitrogen-containing carbon nanotubes, the *O*-configuration being the most stable, probably because the nitrogen atoms are all bonded to carbon atoms, avoiding strong lone-pair–lone-pair repulsions. At the same time, this configuration allows for the development of a positive charge on C2, which theoretically favours nanotube catalytic properties for oxygen reduction reactions.

Hydrogen chemisorption energies for open nitrogen-containing carbon nanotubes ended by hydrogen atoms and similar nanotubes closed at both ends with different units were found to be exothermic and independent of both configuration and length, except for shorter nanotubes.

Chemisorption increases the band gaps ($E_{\text{LUMO}} - E_{\text{HOMO}}$) of the studied nanostructures (from 1–1.6 eV to 4.5–6.5 eV). These band-gap values decrease by approximately 0.4 eV and 1.6 eV, respectively, for nitrogen and phosphorus terminal groups when compared with open saturated nanotubes without terminal groups. Unsaturated nanotube band gaps are insensitive to terminal groups and length.

The dipole moments of saturated nitrogen-containing carbon nanotubes depend more on the tube length than on the type of terminal group, with a variation within 2–3 D for the different end-groups at the considered lengths. In general, the dipole moment increases as the number of layers increases. This finding is also true for open saturated nitrogen-containing carbon nanotubes of different configurations ended by hydrogen atoms. *S*-configuration nanotubes behave as the most polar, and *M*-configuration nanotubes behave as the most unpolar, among all the studied nanotubes, regardless of terminal group.

Nitrogen-containing carbon nanotubes with small diameters have the capacity to store a full monolayer of hydrogen via chemisorption. Shorter nanotubes and nanotubes without end-groups have higher capacities for hydrogen storage. Hydrogen physisorption studies on these nitrogen-containing carbon nanotubes and the effect of increasing the nanotube diameter constitute an important next step.

Important remaining goals are related to the molecular modelling methods and tools necessary for predicting the properties a particular nanostructure will have –as a hydrogen-storage material, a conductive material, a catalyst, or a further functionalisation centre– which continues to be a scientifically interesting and challenging task.

5. Acknowledgements

This work was partially supported by the Direction of Scientific and Technological Research DICYT-USACH project Nr 061042CF and by the SDT-USACH project Nr CIA 2981. Additionally, the central cluster of the Faculty of Chemistry and Biology and the VRID of the University of Santiago de Chile, Usach, are acknowledged for allocating computational resources.

6. References

- Alam, K.M. & Ray, A.K. (2007). A hybrid density functional study of zigzag SiC nanotubes. *Nanotechnology*, Vol.18, No.49 (November 2007) 4957061
- Allen, B.L.; Kichambare, P.D. & Star, A. (2008). Synthesis, characterization, and manipulation of nitrogen-doped carbon nanotube cups. *ACS Nano*, Vol.2, No.9, (September 2008), pp. 1914-1920, ISSN 1936-0851
- Baughman, R.H.; Zakhidov, A.A. & de Heer, W.A. (2002). Carbon nanotubes - the route toward applications. *Science*, Vol.297, No.5582, (August 2002), pp. 787-792, ISSN 0036-8075
- Becke, A.D.J. (1993). Density-functional thermochemistry. 3. The role of exact exchange. *Journal of Chemical Physics*, Vol.98, No.7, pp. 5648-5652, ISSN 0021-9606
- Bilic, A. & Gale, J.D. (2008). Chemisorption of molecular hydrogen on carbon nanotubes: a route to effective hydrogen storage? *Journal of Physical Chemistry C*, Vol.112, No.32, (July 2008), pp. 12568-12575, ISSN 1932-7447
- Cabria, I.; Lopez, M.J. & Alonso, J.A. (2006). Density functional study of molecular hydrogen coverage on carbon nanotubes. *Computational Materials Science*, Vol.35, No.3, (March 2006), pp. 238-242, ISSN 0927-0256
- Charlier, J.C. (2002). Defects in carbon nanotubes. *Accounts of Chemical Research*, Vol.35, No.12, (December 2002), pp. 1063-1069, ISSN 0001-4842
- Contreras, M.L.; Avila, D., Alvarez, J. & Rozas, R. (2010). Exploring the structural and electronic properties of nitrogen-containing exohydrogenated carbon nanotubes: a quantum chemistry study. *Structural Chemistry*, Vol.21, No.3, (June 2010), pp. 573-581, ISSN 1040-0400
- Contreras, M.L.; Benítez, E.; Alvarez, J. & Rozas, R. (2009). Algorithm for nanotubes computer generation with different configurations. *Algorithms*, Vol.2, No.1, (February 2009), pp 108-120, EISSN 1999-4893
- Czerw, R.; Terrones, M.; Charlier, J.C.; Blase, X.; Foley, B.; Kamalakaran, R.; Grobert, N.; Terrones, H.; Ajayan, P.M.; Blau, W.; Tekleab, D.; Rühle, M. & Carroll, D.L. (2001). Identification of electron donor states in N-doped carbon nanotubes. *Nano Letters*, Vol.1, No.9, (September 2001), pp. 457-460, ISSN 1530-6984
- De Jonge, N.; Doytcheva, M.; Allieux, M.; Kaiser, M.; Mentink, S.A.M.; Teo, K.B.K.; Lacerda, R. G. & Milne, W.I. (2005). Cap closing of thin carbon nanotubes. *Advanced Materials*, Vol.17, No.4, (February 2005), pp. 451-455, ISSN 0935-9648
- Dillon, A.C.; Jones, K.M.; Bekkedahl, T.A.; Kiang, C.H.; Bethune, D.S. & Heben, M.J. (1997). Storage of hydrogen in single-walled carbon nanotubes. *Nature*, Vol.386, No.6623, (March 1997), pp. 377-379, ISSN 0028-0836
- Dinadayalane, T.C.; Kaczmarek, A.; Łukaszewicz, J. & Leszczynski, J. (2007). Chemisorption of hydrogen atoms on the sidewalls of armchair single-walled carbon nanotubes.

- Journal of Physical Chemistry C*, Vol.111, No.20, (May 2007), pp. 7376-7383, ISSN 1932-7447
- Feng, H.; Ma, J. & Hu, Z. (2010). Nitrogen-doped carbon nanotubes functionalized by transition metal atoms: a density functional study. *Journal of Materials Chemistry*, Vol.20, No.9, (January 2010), pp. 1702-1708, ISSN 0959-9428
- Frank, S.; Poncharal, P.; Wang, Z.L. & de Heer, W.A. (1998). Carbon nanotube quantum resistors. *Science*, Vol.280, No.5370, (June 1998), pp. 1744-1746, ISSN 0036-8075
- Frisch, M.J.; Trucks, G.W.; Schlegel, H.B.; Scuseria, G.E.; Robb, M.A.; Cheeseman, J.R.; Montgomery, J.A. Jr.; Vreven, T.; Kudin, K.N.; Burant, J.C.; Millam, J.M.; Iyengar, S.S.; Tomasi, J.; Barone, V.; Mennucci, B.; Cossi, M.; Scalmani, G.; Rega, N.; Petersson, G.A.; Nakatsuji, H.; Hada, M.; Ehara, M.; Toyota, K.; Fukuda, R.; Hasegawa, J.; Ishida, M.; Nakajima, T.; Honda, Y.; Kitao, O.; Nakai, H.; Klene, M.; Li, X.; Knox, J.E.; Hratchian, H.P.; Cross, J.B.; Bakken, V.; Adamo, C.; Jaramillo, J.; Gomperts, R.; Stratmann, R.E.; Yazyev, O.; Austin, A.J.; Cammi, R.; Pomelli, C.; Ochterski, J.W.; Ayala, P.Y.; Morokuma, K.; Voth, G.A.; Salvador, P.; Dannenberg, J.J.; Zakrzewski, V.G.; Dapprich, S.; Daniels, A.D.; Strain, M.C.; Farkas, O.; Malick, D.K.; Rabuck, A.D.; Raghavachari, K.; Foresman, J.B.; Ortiz, J.V.; Cui, Q.; Baboul, A.G.; Clifford, S.; Cioslowski, J.; Stefanov, B.B.; Liu, G.; Liashenko, A.; Piskorz, P.; Komaromi, I.; Martin, R.L.; Fox, D.J.; Keith, T.; Al-Laham, M.A.; Peng, C.Y.; Nanayakkara, A.; Challacombe, M.; Gill, P.M.W.; Johnson, B.; Chen, W.; Wong, M.W.; Gonzalez, C. & Pople, J.A (2004). Gaussian 03, Gaussian Inc, Wallingford CT, Revision D01
- Ganji, M.D. (2008). Behavior of a single nitrogen molecule on the pentagon at a carbon nanotube tip: a first-principles study. *Nanotechnology*, Vol.19, No.2, (December 2007), 025709
- Gong, K.P.; Du, Z.H.; Xia, Z.H.; Durstock, M. & Dai, L.M. (2009), Nitrogen-doped carbon nanotube arrays with high electrocatalytic activity for oxygen reduction. *Science*, Vol.323, No.5915, (February 2009), pp. 760-764, ISSN 0036-8075
- Griadun, V. (2010). Doped Carbon Nanotubes Properties, In: *Carbon Nanotubes*, Marulanda, J.M. (Ed), pp. 147-168, In-Teh, ISBN 978-953-307-054-4, India
- Hamada, N.; Sawada, S. & Oshiyama, A. (1992). New one-dimensional conductors-graphitic microtubules, *Physical Review Letters*, Vol.68, No.10, (March 1992), pp. 1579-1581, ISSN 0031-9007
- Han, S.S. & Lee, H.M. (2004). Adsorption properties of hydrogen on (10,0) single-walled carbon nanotube through density functional theory. *Carbon*, Vol.42, No.11, (May 2004) pp. 2169-2177, ISSN 0008-6223
- Hone, J.; Batlogg, B.; Benes, Z.; Johnson, A.T. & Fisher, J.E. (2000). Quantized phonon spectrum of single-wall carbon nanotubes. *Science*, Vol.289, No.5485, (September 2000), pp. 1730-1733, ISSN 0036-8075
- Hu, X.; Zhou, Z.; Lin, Q.; Wu, Y. & Zhang, Z. (2011). High reactivity of metal-free nitrogen-doped carbon nanotube for the C-H activation. *Chemical Physics Letters*, Vol.503, No.4-6, (February 2011), pp. 287-291, ISSN 0009-2614 Hyperchem release 7.0, Hypercube Inc, 1115 NW 4th Street, Gainesville, Florida 32601, USA
- Jaguar version 7.5 (2008) Schrödinger, LLC, New York, NY
- Kang, H.S. & Jeong, S. (2004). Nitrogen doping and chirality of carbon nanotubes, *Physical Review B*, Vol.70, No.23 (December 2004), pp. 233411-1-233411-4. ISSN 1098-0121

- Kang, K.Y.; Lee, B.I. & Lee, J.S. (2009). Hydrogen adsorption on nitrogen-doped carbon xerogels. *Carbon*, Vol.47, No.4, (April 2009), pp. 1171-1180, ISSN 0008-6223
- Kaczmarek, A.; Dinadayalane, T.C.; Łukaszewicz, J. & Leszczynski, J. (2007). Effect of tube length on the chemisorptions of one and two hydrogen atoms on the sidewalls of (3,3) and (4,4) single-walled carbon nanotubes: a theoretical study. *International Journal of Quantum Chemistry*, Vol.107, No.12, (October 2007), pp. 2211-2219, ISSN 0020-7608
- Kovalev, V.; Yakunchikov, A. & Li, F. (2011), Simulation of hydrogen adsorption in carbon nanotube arrays. *Acta Astronautica*, Vol.68, No.7-8, (April-May 2011), pp. 681-685
- Lee, C.; Yang, W. & Parr, R.G. (1988), Development of the colle-salvetti correlation-energy formula into a functional of the electron-density. *Physical Review B*, Vol.37, No.2 (January 1988), pp. 785-789, ISSN 0163-1829
- Liu, C.; Chen, Y.; Wu, C.Z.; Xu, S.T. & Cheng, H.M. (2010). Hydrogen storage in carbon nanostructures revisited. *Carbon*, Vol.48, No.2, (February 2010), pp. 452-455, ISSN 0008-6223
- Marulanda, J.M. (Ed.) (2010). *Carbon Nanotubes*, In-Teh, ISBN 978-953-307-054-4. India
- Mpourmpakis, G.; Tylanakis, E. & Froudakis, G. (2006). Hydrogen storage in carbon nanotubes. A multi-scale theoretical study. *Journal of Nanoscience and Nanotechnology*, Vol.6, No.1, (January 2006), pp. 87-90, ISSN 1533-4880
- Nayak, T.R.; Leow, P.C.; Ee, P.L.R.; Arockiadoss, T.; Ramaprabhu, S. & Pastorin, G. (2010). Crucial parameters responsible for carbon nanotubes toxicity. *Current Nanoscience*, Vol.6, No.2, (April 2010), pp. 141-154 ISSN 1573-4137
- Ni, M.Y. & Zeng, Z. (2010). Chemisorption and diffusion of hydrogen atoms on single-walled carbon nanotubes. *Journal of Nanoscience and Nanotechnology*, Vol.10, No.8, (August 2010), pp. 5408-5412, ISSN 1533-4880
- Oh, K.S.; Kim, D.H.; Park, S.; Lee, J.S.; Kwon, O. & Choi, Y.K. (2008). Movement of hydrogen molecules in pristine, hydrogenated and nitrogen-doped single-walled carbon nanotubes. *Molecular Simulation*, Vol.34, No.10-15, (September-December 2008), pp. 1245-1252, ISSN 0892-7022
- Pastorin, G. (2009). Crucial Functionalizations of Carbon Nanotubes for Improved Drug Delivery: A Valuable Option? *Pharmaceutical Research*, Vol.26, No.4, (April 2009), pp. 746-769, ISSN 0724-8741
- Rangel, E.; Ruiz-Chavarria, G.; Magana, L.F. & Arellano, J.S. (2009). Hydrogen adsorption on N-decorated single wall carbon nanotubes. *Physics Letters A*, Vol.373, No.30, (July 2009), pp. 2588-2591, ISSN 0375-9601
- Saito, R.; Fujita, M.; Dresselhaus, G. & Dresselhaus, M.S. (1992). Electronic-structure of chiral graphene tubules. *Applied Physics Letters*, Vol.60, No.18 (May 1992), pp. 2204-2206, ISSN 0003-6951
- Terrones, M. (2007). Synthesis, toxicity, and applications of doped carbon nanotubes. *Acta Microscopica*, Vol.16, No.1-2 (Suppl. 2), pp. 33-34
- Stern, S.T. & McNeil, S.E. (2008), Nanotechnology safety concerns revisited. *Toxicological Sciences*, Vol.101, No.1, (June 2007), pp. 4-21
- Trasobares, S.; Stephan, O.; Colliex, C.; Hsu, W.K.; Kroto, H.W. & Walton, D.R.M. (2002). Compartmentalized CN_x nanotubes: chemistry, morphology, and growth. *Journal of Chemical Physics*, Vol.116, No.20 (May 2002) pp. 8966-8972, ISSN 0021-9606

- Wang, J.L.; Lushington, G.H. & Mezey, P.G. (2006). Stability and electronic properties of nitrogen nanoneedles and nanotubes. *Journal of Chemical Information and Modeling*, Vol.46, No.5 (September-October 2006), pp.1965-1971 ISSN 1549-9596
- Wang, L.F. & Yang, R.T. (2009). Hydrogen storage properties of N-doped microporous carbon. *Journal of Physical Chemistry C*, Vol.113, No.52, (December 2009), pp. 21883-21888, ISSN 1932-7447
- Xiong, W.; Du, F.; Liu, Y.; Perez, A., Jr.; Supp, M.; Ramakrishnan, T.S.; Dai, L. & Jiang, L. (2010). 3-D carbon nanotube structures used as high performance catalyst for oxygen reduction reaction. *Journal of the American Chemical Society*, Vol.132, No.45, (October 2010), pp.15839-15841, ISSN 0002-7863
- Yang, F.H.; Lachawiec, J., Jr. & Yang, R.T. (2006). Adsorption of spillover hydrogen atoms on single-wall carbon nanotubes. *Journal of Physical Chemistry B*, Vol.110, No.12, (March 2006), pp. 6236-6244, ISSN 1520-6106
- Yang, S.H.; Shin, W.H. & Kang, J.K. (2008). The nature of graphite- and pyridinelike nitrogen configurations in carbon nitride nanotubes: dependence on diameter and helicity. *Small*, Vol.4, No.4, (April 2008), pp. 437-441, ISSN 1613-6810
- Yao, Y. (2010). Hydrogen storage using carbon nanotubes, In: *Carbon Nanotubes*, Marulanda, J.M. (Ed), pp. 543-562, In-Teh, ISBN 978-953-307-054-4, India
- Yu, M.F.; Files, B.S.; Arepalli, S. & Ruoff, R.S. (2000). Tensile loading of ropes of single wall carbon nanotubes and their mechanical properties. *Physical Review Letters*, Vol.84, No.24, (June 2000), pp. 5552-5555, ISSN 0031-9007
- Zhang, G.; Qi, P.; Wang, X.; Lu, Y.; Mann, D.; Li, X. & Dai, H. (2006). Hydrogenation and hydrocarbonation and etching of single-walled carbon nanotubes. *Journal of the American Chemical Society*, Vol.128, No.18, (May 2006), pp. 6026-6027, ISSN 0002-7863
- Zhang, Y.; Wen, B.; Song, X.Y. & Li, T.J. (2010). Synthesis and bonding properties of carbon nanotubes with different nitrogen contents. *Acta Physica Sinica*, Vol.59, No.5, (May 2010), pp. 3583-3588, ISSN 1000-3290
- Zhang, Z. Y. & Cho, K. (2007). Ab initio study of hydrogen interaction with pure and nitrogen-doped carbon nanotubes. *Physical Review B*, Vol.75, No.7, (February 2007), Art. No. 075420, 6 pp., ISSN 1098-0121
- Zhong, Z.; Lee, G.I.; Mo, C.B.; Hong, S.H. & Kang, J.K. (2007). Tailored field-emission property of patterned carbon nitride nanotubes by a selective doping of substitutional N(sN) and pyridine-like N(pN) atoms. *Chemistry and Materials*, Vol.19, No.12 (June 2007), pp. 2918-2920, ISSN: 0897-4756
- Zhou, Z.; Gao, X.P.; Yan, J. & Song, D.Y. (2006). Doping effects of B and N on hydrogen adsorption in single-walled carbon nanotubes through density functional calculations. *Carbon*, Vol.44, No.5, (April 2006), pp. 939-947, ISSN 008-6223



Carbon Nanotubes - From Research to Applications

Edited by Dr. Stefano Bianco

ISBN 978-953-307-500-6

Hard cover, 358 pages

Publisher InTech

Published online 20, July, 2011

Published in print edition July, 2011

Since their discovery in 1991, carbon nanotubes have been considered as one of the most promising materials for a wide range of applications, in virtue of their outstanding properties. During the last two decades, both single-walled and multi-walled CNTs probably represented the hottest research topic concerning materials science, equally from a fundamental and from an applicative point of view. There is a prevailing opinion among the research community that CNTs are now ready for application in everyday world. This book provides an (obviously not exhaustive) overview on some of the amazing possible applications of CNT-based materials in the near future.

How to reference

In order to correctly reference this scholarly work, feel free to copy and paste the following:

Roberto Rozas and M. Leonor Contreras (2011). Nitrogen-Containing Carbon Nanotubes. A Theoretical Approach, Carbon Nanotubes - From Research to Applications, Dr. Stefano Bianco (Ed.), ISBN: 978-953-307-500-6, InTech, Available from: <http://www.intechopen.com/books/carbon-nanotubes-from-research-to-applications/nitrogen-containing-carbon-nanotubes-a-theoretical-approach>

INTECH
open science | open minds

InTech Europe

University Campus STeP Ri
Slavka Krautzeka 83/A
51000 Rijeka, Croatia
Phone: +385 (51) 770 447
Fax: +385 (51) 686 166
www.intechopen.com

InTech China

Unit 405, Office Block, Hotel Equatorial Shanghai
No.65, Yan An Road (West), Shanghai, 200040, China
中国上海市延安西路65号上海国际贵都大饭店办公楼405单元
Phone: +86-21-62489820
Fax: +86-21-62489821

© 2011 The Author(s). Licensee IntechOpen. This chapter is distributed under the terms of the [Creative Commons Attribution-NonCommercial-ShareAlike-3.0 License](#), which permits use, distribution and reproduction for non-commercial purposes, provided the original is properly cited and derivative works building on this content are distributed under the same license.

IntechOpen

IntechOpen